

Quasi-phase-matched second-harmonic generation in a GaAs/AlAs superlattice waveguide by ion-implantation-induced intermixing

K. Zeaiter and D. C. Hutchings

Department of Electronics and Electrical Engineering, University of Glasgow, Glasgow G12 8QQ, Scotland, UK

R. M. Gwilliam

Ion Beam Centre, University of Surrey, Guildford, Surrey GU2 7XH, UK

K. Moutzouris, S. Venugopal Rao, and M. Ebrahimzadeh

School of Physics and Astronomy, University of St. Andrews, St. Andrews, Fife KY16 9SS, Scotland, UK

Received December 9, 2002

We report type I second-harmonic generation by use of first-order quasi-phase matching in a GaAs/AlAs symmetric superlattice structure with femtosecond fundamental pulses at $1.55\ \mu\text{m}$. Periodic spatial modulation of the bulklike second-order susceptibility $\chi_{zxy}^{(2)}$ was achieved with quantum-well intermixing for which the group III vacancies were created by As^+ -ion implantation. A narrow second-harmonic bandwidth of $\sim 0.9\ \text{nm}$ (FWHM) with an average power of $\sim 1.5\ \mu\text{W}$ was detected, corresponding to an internal conversion efficiency of $\sim 0.06\%$, which was considerably limited by the spectral bandwidth of the fundamental. © 2003 Optical Society of America

OCIS codes: 190.5970, 160.4330, 190.2620, 230.7370.

Several techniques for the development of semiconductor waveguides for wavelength conversion that use second-order nonlinearities have been explored. Potential applications include difference-frequency mixing for channel conversion in wavelength-division multiplexing¹ and novel optical sources based on parametric processes. Contemporary approaches to phase matching in semiconductors have generally required definition at the growth stage, for example, to exploit birefringent phase matching by use of selective oxidation² or patterned substrate growth for quasi-phase matching^{3,4} (QPM). Quantum-well intermixing represents a range of techniques developed in recent years, primarily for the postgrowth fabrication of monolithically integrated optoelectronic devices that use quantum wells in their active regions.⁵ The bandgap shift obtained with these techniques also leads to a modification of the nonlinear optical properties, which can be exploited to produce QPM of second-order nonlinear processes. The postgrowth QPM fabrication techniques that use intermixing offer greater flexibility than other phase-matching schemes in III–V semiconductor waveguides. Standard growth techniques are used, which both permit the grating period to be subsequently lithographically defined and allow the possibility of direct integration with a pump diode laser.

The motivation for the present study also stems from the fact that although there have been two recent demonstrations of second-harmonic generation (SHG) by use of QPM through intermixing, the processes were characterized by low efficiencies. Using the sputtered silica cap disordering technique in GaAs/AlAs superlattice waveguides has produced third-order quasi-phase-matched SHG based on modulation in the bulklike $\chi_{zxy}^{(2)}$ coefficient under type I interaction.⁶ The magnitude of this modulation in the bulklike

second-order susceptibility in GaAs/AlAs superlattices was predicted to be as large as those attained in periodically poled LiNbO_3 .⁷ However, the sample processing required for the necessary micrometer-scale resolution has been difficult to reproduce, and improvements in conversion efficiency have proved elusive in spite of extensive process development and optimization.⁸ These fabrication limitations may be unavoidable, as the sputtered silica process creates group III vacancies at the wafer surface, which then have to migrate across the waveguide cladding and the core regions to promote intermixing; some lateral spreading is inevitable. Previous reports indicate the necessity for obtaining the spatial resolution required for first-order gratings, even if higher-order gratings are used.⁹ Bouchard *et al.*¹⁰ used ion-implantation-induced intermixing¹¹ in an asymmetric AlGaAs quantum-well waveguide based on modulation in the induced, but far smaller, $\chi_{zzz}^{(2)}$ coefficient. Attempts to observe QPM SHG based on the larger absolute modulation in the bulklike $\chi_{zxy}^{(2)}$ coefficient, however, proved unsuccessful. Here we present new results with first-order QPM SHG based on ion-implantation induced intermixing with the larger modulation obtained with the bulklike $\chi_{zxy}^{(2)}$ coefficient. The improvement in the conversion efficiency enabled us to simply use a commercial powermeter for detection of the second-harmonic (SH) signal.

For a fundamental wavelength at $1.5\ \mu\text{m}$, the period of the first-order grating was calculated to be $\sim 3.7\ \mu\text{m}$ by use of the effective refractive-index data measured with a coupler grating technique.¹² A rib waveguide structure was used to maintain the fundamental and SH intensities and their overlap over a sufficient distance for the nonlinear process to proceed efficiently. The layer structure of the sample used in the present study is identical to that described in Ref. 9

and consists of a 0.6- μm core of GaAs/AlAs superlattice that comprises 75 periods of 14:14 monolayers and is clad on either side with a 0.3- μm $\text{Al}_{0.56}\text{Ga}_{0.44}\text{As}$ buffer layer. The lower and upper cladding layers were bulk $\text{Al}_{0.6}\text{Ga}_{0.4}\text{As}$ with 4- and 0.8- μm thickness, respectively, and capped with 100 nm of GaAs. The structure was nominally undoped, grown by molecular beam epitaxy upon a semi-insulating (100) GaAs substrate. The room-temperature photoluminescence emission wavelength of the structure was 750 nm from the central portion of the wafer. This design allows the operating fundamental wavelength, ~ 1550 nm, at 30 meV below the half-bandgap to avoid two-photon absorption and use the modulation attained in the resonant component of $\chi^{(2)}$ as the bandgap of the structure is shifted.

The QPM grating was achieved with As^+ -ion implantation to prevent the introduction of any impurity defects into the material. A Transport of Ions in Matter software simulation predicted that an ion energy of 4 MeV would correspond to an ion range of 1.7 μm and a lateral straggle of 0.45 μm , which are adequate for the creation of group III vacancies in the superlattice layers while the desired spatial resolution is maintained. The incident ion beam was tilted by 7° to prevent a channelling effect that would increase the damage incurred within the lattices and hence modify the intermixing process. A gold mask of ~ 1.5 - μm thickness, which was predicted to be sufficient to protect the desired regions from the As^+ ions, was grown by electroplating. A sealing layer of 4-nm Au and 30-nm Ti followed by 40-nm sputtered Au was grown on the sample surface and was connected to the electrode by a metallic contact (Ag in methyl isobutyl ketone). An electron-sensitive photoresist layer of PMMA of ~ 3 - μm thickness was then spun on top of the sample, and the QPM pattern was transferred to the photoresist (insulator) layer by electron-beam lithography. After developing, the sample was submerged in a Au solution (sulfite gold), where electric tension was applied. Once the Au pattern was grown, the photoresist was stripped off with hot acetone. After implantation, the Au mask was removed by wet etching in a solution of potassium iodide. The sample was annealed face down in a rapid thermal annealer at 850°C for 30 s. Figure 1 shows the photoluminescence peak wavelength blueshift in the large-area intermixed samples in comparison to the as-grown sample as a function of ion flux and approaches saturation for a dosage of 10^{13} – 10^{14} ions/ cm^2 . High ion dosages would substantially increase optical losses caused by amorphism. Strip-loaded rib waveguides were fabricated by reactive-ion etching, and the sample was cleaved on each side. A loss measurement at a wavelength of 1.55 μm , based on a Fabry-Perot technique, yielded a value of ~ 21 dB/cm in the quasi-phase-matched sample implanted with an ion dosage of 10^{14} ions/ cm^2 , which we employed in the nonlinear measurements reported as follows.

The optical source used for the SHG experiments was a synchronously pumped, femtosecond optical parametric oscillator (OPO) based on periodically

poled lithium niobate in a semimonolithic cavity design. An average power of ~ 80 mW was routinely available from the OPO in pulses of ~ 250 -fs duration at an ~ 90 -MHz repetition rate. A 2-mm-long sample with a first-order grating period was mounted upon an end-fire coupling rig. Linearly polarized light from the OPO was launched into the waveguide, with the output of the waveguides aligned onto a semiconductor powermeter. A typical measurement of the SH spectra, obtained with an optical spectrum analyzer, is shown in Fig. 2. As expected for type I phase matching, the detected SH signal was TM polarized with a TE fundamental polarization. There was no SH signal detected for a TM-polarized fundamental. The measured bandwidth of the fundamental was ~ 10 nm (FWHM), whereas that of the SH, determined by the finite bandwidth of the QPM grating, was ~ 0.9 nm. The SHG signal appeared only when the output spectrum of the OPO was tuned to provide the appropriate wavelength for the QPM grating under test. By tuning the pump away from the phase-matching wavelength we also observed a broad-bandwidth non-phase-matched signal at lower power levels, as is depicted in the inset of Fig. 2, where the fundamental was detuned by ~ 10 nm with respect to the optimal phase-matching wavelength.

The measured average SHG power is plotted in Fig. 3(a) as a function of peak fundamental wavelength. As the source is not monochromatic, the line shape is determined by the fundamental spectrum

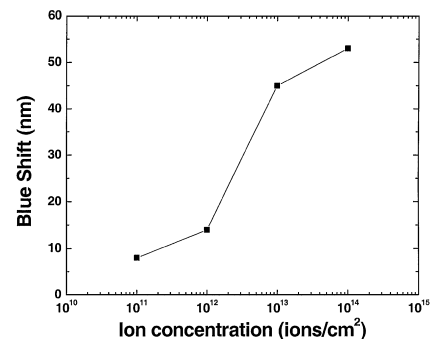


Fig. 1. Photoluminescence (at 77 K) blueshift as a function of As^+ -ion flux at 4-MeV energy. Samples were annealed at 850°C for 30 s.

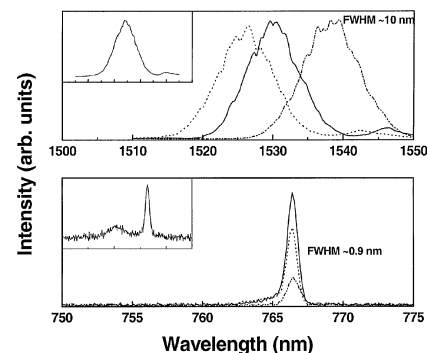


Fig. 2. Observed SH (bottom) and fundamental (top) spectra. Insets, corresponding spectra on an expanded vertical scale at a detuning of 10 nm; both phase-matched and non-phase-matched components are evident.

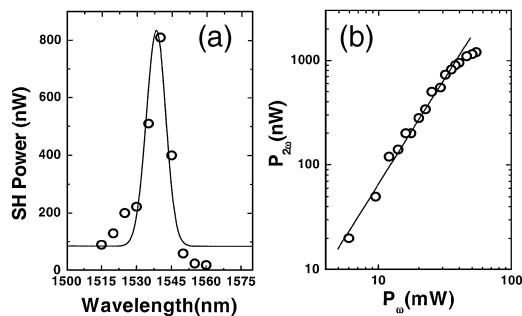


Fig. 3. (a) Measured wavelength-tuning curve for SHG by a femtosecond optical source. (b) SH output average power as a function of the fundamental input average power on a log-log scale. The best fit to the slope is 2.04, confirming the expected quadratic power dependence.

rather than by the usual sinc^2 function. We fitted the wavelength-tuning curve to a Gaussian on a pedestal corresponding to the square of the fundamental spectrum and a non-phase-matched component. Figure 3(b) shows a typical result of the dependence of the average SH power on the fundamental power. The best fit to the slope on a log-log plot was 2.04, confirming the expected quadratic power dependence. Saturation of the SHG power started at ~ 40 mW of input power. As the grating period decreased, the phase-matched SHG signal shifted to shorter wavelengths, as expected with normal dispersion. The lower wavelength limit was reached when SH photon energy approached the material bandgap and experienced excessive band-edge absorption. Using longer grating periods, we were also able to observe third-order QPM with an appropriate drop in the generate SH power levels.

The use of a femtosecond source introduces several unknown factors (see below) in the determination of conventional conversion efficiencies. However, we were able to make comparisons with previous experiments by noting that the largest SHG average power measured was $1.5 \mu\text{W}$ at a wavelength of 767 nm. Taking into account the estimated 5-dB loss between waveguide and detector and the 30% reflection loss at the rear facet of the waveguide, we estimated an average SHG power of $\sim 7 \mu\text{W}$ generated within the waveguide. The average power in the transmitted fundamental was ~ 2.9 mW, which, with a 30% loss at the rear facet and a measured optical loss of ~ 21 dB/cm in the waveguide, translates to an average pump power of ~ 11 mW just after the front facet of the waveguide and thus corresponds to an end-fire coupling efficiency of $\sim 18\%$. Hence we obtained a maximum SHG conversion of $\sim 0.06\%$ with the present setup, for which there is considerable scope for improvement: (1) The femtosecond source is not ideal, as it has a bandwidth much larger than the QPM grating and dispersion will also result in significant temporal broadening of the fundamental pulse. (2) Defect outdiffusion and ion implantation lateral straggle will modify the QPM grating from the ideal 50:50 square wave. (3) The optical losses are slightly high compared with those for other intermixed

waveguides, which may be due partly to surface damage caused by the Au etch, so an additional protective SiO_2 layer will be added to future samples. It may also be desirable to use a lower ion dosage to trade off some of the modulation of the nonlinear coefficient for lower losses. (4) Furthermore, it has been predicted that the associated modulation in the linear refractive index ($\Delta n \sim 0.01$ has been measured at $\lambda \sim 1550$ nm for this wafer structure intermixed by the sputtered silica cap process¹²) will also compromise conversion efficiency by $\sim 30\%$.^{13,14}

We have demonstrated SHG under type I QPM in GaAs/AlAs superlattice waveguides by the use of a first-order grating. We achieved QPM through modulation of the bulklike nonlinear coefficient, $\chi^{(2)}$, by periodically tuning the superlattice bandgap with quantum-well intermixing induced by As⁺-ion implantation.

This research was supported by grant GR/M78939 from the Engineering and Physical Sciences Research Council (UK). D. C. Hutchings's e-mail address is d.hutchings@elec.gla.ac.uk.

References

1. S. J. B. Yoo, *J. Lightwave Technol.* **14**, 955 (1996).
2. K. Moutzouris, S. Venugopal Rao, M. Ebrahimzadeh, A. De Rossi, V. Berger, M. Calligaro, and V. Ortiz, *Opt. Lett.* **26**, 1785 (2001), and references therein.
3. S. J. B. Yoo, R. Bhat, C. Caneau, and M. A. Koza, *Appl. Phys. Lett.* **66**, 3410 (1995).
4. L. A. Eyres, P. J. Tourreau, T. J. Pinguet, C. B. Ebert, J. S. Harris, M. M. Fejer, L. Becouarn, B. Gerard, and E. Lallier, *Appl. Phys. Lett.* **79**, 904 (2001).
5. For example, E. H. Li, E. S. Koteles, and J. H. Marsh, eds., special issue on interdiffused quantum-well materials and devices, *IEEE J. Sel. Top. Quantum Electron.* **4**(4) (1998).
6. A. Saher-Helmy, D. C. Hutchings, T. C. Kleckner, J. H. Marsh, A. C. Bryce, J. M. Arnold, C. R. Stanley, J. S. Aitchison, C. T. A. Brown, K. Moutzouris, and M. Ebrahimzadeh, *Opt. Lett.* **25**, 1370 (2000).
7. D. C. Hutchings, *Appl. Phys. Lett.* **76**, 1362 (2000).
8. K. Zeaiter, T. C. Kleckner, J. S. Aitchison, and D. C. Hutchings, in *Nonlinear Guided Waves and Their Applications*, Vol. 80 of OSA TOPS (Optical Society of America, Washington, D.C., 2002), paper MD37.
9. D. C. Hutchings and T. C. Kleckner, *J. Opt. Soc. Am. B* **19**, 890 (2002).
10. J.-P. Bouchard, M. Tetu, S. Janz, D. X. Xu, Z. R. Wasilewski, P. Piva, U. G. Akano, and I. V. Mitchell, *Appl. Phys. Lett.* **77**, 4247 (2000).
11. H. Leier, A. Forchel, G. Horcher, J. Hommel, S. Bayer, H. Rothfritz, G. Weimann, and W. Schlapp, *J. Appl. Phys.* **67**, 1805 (1990).
12. T. C. Kleckner, "Quasi-phase-matched nonlinear frequency conversion in periodically disordered GaAs/AlAs superlattice-core waveguides," Ph.D. dissertation (University of Glasgow, Glasgow, Scotland, 2002).
13. C. De Angelis, F. Gringoli, M. Midrio, D. Modotto, J. S. Aitchison, and G. F. Nalesso, *J. Opt. Soc. Am. B* **18**, 348 (2001).
14. D. Modotto, University of Glasgow (personal communication, 2001).